

Simulation of Electrochemical Aptamer-Based Sensors: A Kinetic and Binding Model Perspective

A Haghighatbin

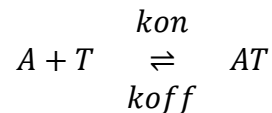
Electrochemical aptamer-based sensors represent a rapidly evolving class of biosensors that exploit the specific binding properties of nucleic acid aptamers to detect target molecules. The operation of these sensors is intrinsically linked to the conformational dynamics of the aptamer and its subsequent modulation of electron transfer kinetics. This article provides an overview of the simulation of such sensors, detailing the derivation of the governing kinetic equations, the relationship between these equations and the Hill–Langmuir isotherm, and the factors that contribute to the characteristic sigmoidal binding curves observed in experimental data. By integrating fundamental principles of chemical kinetics with established binding models, the simulation framework elucidates the operational mechanisms of these sensors and offers insight into their optimisation and performance evaluation.

Electrochemical aptamer-based sensors have emerged as a significant technological innovation in the field of biosensing. Unlike conventional antibody-based systems, aptamers are synthetic oligonucleotides that can be engineered to recognise a wide array of targets, including proteins, small molecules, and even cells. Their stability, ease of synthesis, and capacity for conformational modulation upon target binding render them particularly attractive for incorporation into electrochemical sensing platforms. The core principle of these sensors lies in the translation of a molecular recognition event into a measurable electrical signal, primarily through changes in electron transfer rates induced by aptamer conformational changes.

Understanding and simulating the behaviour of electrochemical aptamer-based sensors is crucial for advancing their design and application. Simulation not only allows for the prediction of sensor responses under various conditions but also aids in the optimisation of sensor parameters, such as binding kinetics and electron transfer efficiency. In this context, the derivation of the underlying kinetic equations and the incorporation of binding models such as the Hill–Langmuir isotherm is fundamental to a robust simulation framework.

Kinetic Modelling of Aptamer–Target Interactions

At the heart of the simulation of electrochemical aptamer-based sensors is the kinetic model that describes the binding interaction between the aptamer and its target. The reaction is typically represented as a simple reversible binding process:



Here, A denotes the aptamer, T represents the target molecule, and AT is the aptamer–target complex. The rate constants k_{on} and k_{off} govern the forward (binding) and reverse (dissociation) reactions, respectively.

The application of the law of mass action to this system stipulates that the rate of the forward reaction is proportional to the product of the concentrations of the free aptamer and the target:

$$\text{Rate}_{\text{forward}} = k_{\text{on}} \cdot [A] \cdot [T]$$

Similarly, the rate of dissociation is proportional to the concentration of the formed complex:

$$\text{Rate}_{\text{reverse}} = k_{\text{off}} \cdot [\text{AT}]$$

Thus, the net rate of formation of the complex $[\text{AT}]$ is given by the difference between these two rates:

$$\frac{d[\text{AT}]}{dt} = k_{\text{on}} \cdot [\text{A}] \cdot [\text{T}] - k_{\text{off}} \cdot [\text{AT}]$$

To account for the conservation of the total aptamer concentration, we introduce A_{Total} where

$$A_{\text{total}} = [\text{A}] + [\text{AT}]$$

Thus, the concentration of free aptamer is expressed as:

$$[\text{A}] = A_{\text{total}} - [\text{AT}]$$

Substituting this into the net rate equation yields:

$$\frac{d[\text{AT}]}{dt} = k_{\text{on}} \cdot (A_{\text{total}} - [\text{AT}]) \cdot [\text{T}] - k_{\text{off}} \cdot [\text{AT}]$$

This differential equation forms the cornerstone of the simulation model, capturing the time-dependent kinetics of the aptamer–target binding process. While the differential equation derived above provides a dynamic description of binding, its steady-state solution is intimately connected to the well-known Hill–Langmuir isotherm. At equilibrium, where $\frac{d[\text{AT}]}{dt} = 0$ the rate of association equals the rate of dissociation:

$$k_{\text{on}} \cdot (A_{\text{total}} - [\text{AT}]) \cdot [\text{T}] = -k_{\text{off}} \cdot [\text{AT}]$$

Rearranging this equation allows one to solve for the equilibrium concentration $[\text{AT}]_{\text{eq}}$

$$[\text{AT}]_{\text{eq}} = \frac{k_{\text{on}} A_{\text{total}} [\text{T}]}{k_{\text{off}} + k_{\text{on}} [\text{T}]}$$

The fraction of aptamers that are bound at equilibrium, defined as θ , is then:

$$\theta = \frac{[\text{AT}]_{\text{eq}}}{A_{\text{total}}},$$

where the dissociation constant K_d is given by:

$$K_d = \frac{k_{\text{off}}}{k_{\text{on}}}$$

Hence,

$$\theta = \frac{[\text{AT}]_{\text{eq}}}{A_{\text{total}}} = \frac{[\text{T}]}{K_d + [\text{T}]}$$

This expression is recognised as the classical Hill–Langmuir isotherm, which is a special case of the more general Langmuir equation. In scenarios where the binding is non-cooperative (i.e. the binding of one molecule does not influence the binding of another), the Hill coefficient n is equal to 1, and the binding curve is hyperbolic. However, if cooperative binding is present, the Hill–Langmuir isotherm takes the form:

$$\theta = \frac{[AT]_{eq}}{A_{total}} = \frac{[T]^n}{K_d^n + [T]^n}.$$

The introduction of the Hill coefficient n allows for the modelling of sigmoidal binding curves, which are often observed when multiple binding sites or cooperative interactions are involved. This sigmoidal behaviour is a direct manifestation of the underlying cooperative mechanisms that govern the sensor's response to varying target concentrations.

In simulating the behaviour of electrochemical aptamer-based (E-AB) sensors, the dynamic evolution of the aptamer–target complex is typically modelled by solving the relevant time-dependent differential equations, as previously derived. The resulting electrochemical current, corresponding to the target concentration, is commonly modelled as a function of the fraction of bound aptamers. In its simplest form, a linear dependency is assumed:

$$I = I_{min} + (I_{max} - I_{min}) \cdot \theta$$

Incorporating cooperative or non-cooperative binding behaviour, the Hill coefficient (n), refines this expression to:

$$I = I_{min} + (I_{max} - I_{min}) \cdot \frac{[T]^n}{K_d^n + [T]^n}$$

In this expression, I_{min} and I_{max} correspond to the baseline and saturated current responses, respectively, while $[T]$ denotes the target concentration and K_d is the apparent dissociation constant. As $\theta \rightarrow 1$, the current asymptotically approaches I_{max} , whereas in the limit $\theta \rightarrow 0$, the current converges to I_{min} . The overall current response versus target concentration retains a sigmoidal profile, shaped by the degree of cooperativity.

It is noteworthy that even in the absence of cooperative binding (i.e., $n = 1$), plotting the current response against the logarithm of the target concentration produces an apparent sigmoidal trend. This phenomenon arises from the logarithmic transformation, which compresses low-concentration data and amplifies mid-range transitions, thereby enhancing the visual transition between unbound and bound states. This effect must be carefully considered when interpreting simulated data or fitting experimental results to the Hill–Langmuir model.

While the model described above provides a convenient and conceptually elegant method to relate the electrochemical current to the binding fraction, it inevitably overlooks a range of physical and electrochemical subtleties. It is, in essence, an idealisation—a static snapshot attempting to describe a dynamic electrochemical process. In practice, electron transfer kinetics, molecular motion, and interfacial phenomena all contribute to the observed signal, and their neglect may result in oversimplified or inaccurate parameter estimations. Several key phenomena merit particular attention when simulating or interpreting current responses in “signal-on” E-AB sensors, wherein the aptamer folds upon target recognition, bringing the redox reporter (e.g., methylene blue) into closer proximity with the electrode surface:

1. **Aptamer Conformational change:** Upon target binding, aptamers undergo a conformational change that repositions the redox reporter, typically from a distal to a proximal state, in a signal-on mechanism, relative to the electrode and vice versa in a signal-off mechanism. This molecular bending modulates the distance-dependent electron tunnelling rate between the redox label and the electrode. Given the exponential dependence of electron transfer rate on distance (as per Marcus theory), even modest

changes in spatial separation can lead to orders-of-magnitude variation in the observed current.

2. **Electron-Transfer Kinetics (Redox Reaction at the Electrode):** Electron transfer at the electrode–redox label interface underpins the faradaic signal in E-AB sensors. In the bound state, the redox moiety (e.g., methylene blue) is oriented closer to the gold electrode, facilitating faster electron exchange. Conversely, in the unbound conformation, the increased distance and unfavourable orientation slow the electron transfer process. These kinetics are typically modelled using either the Butler–Volmer formalism or, for more accurate distance-dependence, the Marcus–Hush–Chidsey approach. The electron transfer event occurs on a timescale of microseconds to milliseconds and is sensitive to both aptamer orientation and surface density.
3. **Double-Layer Charging or Interfacial Capacitance:** All electrochemical measurements at polarised interfaces are influenced by the formation of an electrical double layer. Upon application of a potential, a non-faradaic charging current arises due to the rearrangement of ions in the vicinity of the electrode surface. This double layer behaves as a capacitor, and its charging or discharging competes with the faradaic current. The influence of this phenomenon is particularly pronounced when using Square Wave Voltammetry (SWV), where high-frequency perturbations can result in significant capacitive currents. These capacitive contributions may obscure or distort the true faradaic signal, especially when surface coverage of aptamers varies or when measurements are conducted at different ionic strengths. The decay of the capacitive current is often incorporated into simulation models via frequency-dependent components or baseline correction terms.
4. **Mass Transport (Diffusion, Convection):** Although E-AB sensors often immobilise the aptamer and covalently tether the redox label, mass transport remains relevant, particularly for the target analyte. In stagnant conditions, the diffusion of target molecules toward the electrode may become rate-limiting, especially at low concentrations or in low-conductivity media. Moreover, repetitive scanning or prolonged exposure may induce local depletion zones or concentration gradients. These effects may be exacerbated under high-frequency interrogation regimes, introducing deviations from idealised binding kinetics.
5. **Non-Specific Adsorption or Partial Blocking:** The electrochemical interface is susceptible to contamination and adsorption of extraneous species, which may competitively inhibit aptamer function or alter the effective electroactive surface area. Adsorption of non-specific proteins, ions, or degradation products may partially block electron transfer pathways, while conformational rearrangements or packing effects of aptamers over time can further complicate signal interpretation. These phenomena often manifest as a slow temporal drift or reduced sensitivity, necessitating rigorous control experiments and surface regeneration protocols.

Whilst the aforementioned processes contribute to the overall electrochemical signal, the relative significance of each in practice can vary considerably. Consequently, when constructing a simulation framework, it is both reasonable and often necessary to omit those phenomena whose contributions are minimal or experimentally indistinguishable from

baseline variation. For instance, in systems where double-layer capacitance is well characterised and stable, or where non-specific adsorption is minimised through rigorous surface preparation, these contributions may be treated as negligible.

Nevertheless, it must be acknowledged that not all aptamer–target interactions adhere to a simple two-state model. In certain cases, aptamers undergo multi-step conformational transitions, progressing through intermediate folding states before achieving the final, target-bound conformation. These structural intermediates can give rise to complex kinetic behaviour, with distinct time constants characterising each conformational transition. In frequency-sweep electrochemical experiments, such as SWV conducted across a range of frequencies, these events may manifest as multiple exponential decay components in the current response—each corresponding to a discrete dynamic process, such as an initial partial fold followed by final anchoring to the electrode surface.

Although such mechanisms are biologically and chemically plausible, incorporating them into a generalised simulation framework substantially increases model complexity, requiring additional parameters that may not be easily constrained experimentally. For the purposes of this discussion, and in line with conventional modelling approaches, such intermediate states are excluded. Their rigorous treatment is best reserved for detailed kinetic investigations beyond the scope of the present model.

In the canonical representation of E-AB sensor response—typically applied under equilibrium conditions or at a fixed interrogation frequency—the relationship between current and target concentration is captured by:

$$I = I_{\min} + (I_{\max} - I_{\min}) \theta, \quad \theta = \frac{[T]}{K_D + [T]}$$

This model succinctly describes the transition in the measured current from I_{\min} , representing the fully unbound state, to I_{\max} , corresponding to complete aptamer saturation assuming a one-to-one binding stoichiometry and non-cooperative interaction ($n = 1$). However, this formulation does not account for the frequency dependence of the sensor's output in techniques such as Square Wave Voltammetry (SWV). In practice, when the sensor is interrogated across a spectrum of frequencies, both the unbound and saturated states yield distinct, frequency-dependent current responses. These are shaped not only by the fundamental electron transfer kinetics but also by the finite temporal resolution imposed by the square wave perturbation—specifically, the limited duration available in each half-cycle of the square wave signal.

To address these limitations and accurately describe the sensor's performance under dynamic interrogation, more sophisticated models are introduced. These consider the interplay between binding kinetics, electron transfer rates, and the time constant associated with the applied frequency. In such models, the observed amplitude of the current (whether expressed as peak height or integrated charge) is modulated by:

- The duration of each half-cycle in SWV, which constrains the system's ability to reach steady state before the direction of potential is reversed;
- The rate of electron transfer, governed by the spatial arrangement of the redox label and its tunnelling efficiency;

- The capacitive behaviour of the electrode–solution interface, particularly at higher frequencies where capacitive charging may dominate the current response.

Such frequency-sensitive models are essential for capturing the full dynamic range of E-AB sensors and for fitting data collected under non-equilibrium or time-resolved conditions. Incorporating these considerations enables a more accurate deconvolution of faradaic and non-faradaic components and enhances the fidelity of parameter estimation in sensor calibration and optimisation studies. A simple phenomenological version uses multiple exponential “penalties” in series:

$$I_{\text{net}}(f) = I_0 \exp\left(-\frac{k_{\text{et}}}{2f}\right) \cdot \exp\left(-\frac{f}{f_{\text{conf}}}\right) \cdot \exp\left(-\frac{f}{f_{\text{DL}}}\right) \cdot \exp\left(-\frac{f}{f_{\text{mass}}}\right) \cdot \exp\left(-\frac{f}{f_{\text{ads}}}\right)$$

Where:

- I_0 is an overall scaling factor (could also be fitted).
- $\exp(-k_{\text{et}}/(2f))$ captures the electron-transfer kinetics that often appear in SWV modelling (the $1/(2f)$ factor is a heuristic).
- $\exp(-f/f_{\text{conf}})$ could be a rough proxy for how aptamer conformational gating becomes less effective at higher frequencies (there’s less time for the aptamer to fold “signal-on”).
- $\exp(-f/f_{\text{DL}})$ the effect of double-layer charging at high frequencies.
- $\exp(-f/f_{\text{mass}})$ might account for mass-transport or diffusion limitations.
- $\exp(-f/f_{\text{ads}})$ could represent partial blocking or slow fouling processes that reduce the current with increasing frequency.

To incorporate the dynamic effects observed in frequency-dependent interrogation methods such as Square Wave Voltammetry (SWV), and in order to strike a balance between physical accuracy and computational tractability, a simplified yet physically insightful model can be employed. Recognising that conformational dynamics f_{conf} typically exert a dominant influence on signal modulation, while contributions from double-layer capacitance f_{DL} , mass transport f_{mass} and surface adsorption f_{ads} are comparatively minor under controlled experimental conditions, the model may be parameterised as follows:

$$I_{\text{net}}(f) = I_0 \exp\left(-\frac{k_{\text{et}}}{2f}\right) \cdot \exp\left(-\frac{f}{f_{\text{conf}}}\right) \cdot \exp\left(-\frac{f}{f_{\text{others}}}\right),$$

where $I_{\text{net}}(f)$ represents the net frequency-dependent current response, I_0 is the baseline amplitude in the low-frequency regime, analogous to I_{min} or I_{max} depending on the bound state, k_{et} is the effective electron transfer rate constant, governing the rate-limiting kinetics of the redox event, f_{conf} denotes the characteristic frequency associated with aptamer conformational dynamics, representing a gating process whereby higher frequencies outpace the aptamer’s ability to reconfigure, f_{others} encapsulates secondary decay channels, including double-layer effects f_{DL} , mass transport limitations f_{mass} , and non-specific adsorption or surface passivation effects f_{ads} . Therefore, the first term $\exp(-k_{\text{et}}/(2f))$, represents the attenuation of the current due to finite electron transfer rates—a phenomenon well described in the context of tunnelling-limited kinetics and consistent with Marcus-type behaviour, where faster square-wave cycles

diminish the likelihood of successful redox events, and $\exp\left(-\frac{f}{f_{\text{conf}}}\right) \cdot \exp(-f/f_{\text{others}})$ lumps together phenomena such as conformational gating and residual non-idealities such as double-layer charging, mass transport, and adsorption/passivation effects grouped under f_{others} .

Practically, a distinct set of parameters $\{I_0, k_{\text{et}}, f_{\text{conf}}, f_{\text{others}}\}$ can be fitted for each aptamer state (unbound vs. bound). This parameterisation permits the reconstruction of two characteristic frequency-sweep curves—one corresponding to the absence of target and one to saturation with target. These curves may be generated either experimentally or via simulation and subsequently used to calibrate the model. In the low-frequency limit $f \ll f_{\text{conf}}, f_{\text{others}}$ all exponential terms asymptotically approach unity:

$$\lim_{f \rightarrow 0} I_{\text{net}}(f) = I_0$$

Under such conditions, the sensor response approaches a steady-state amplitude equivalent to the equilibrium-bound value, reaffirming the equivalence between time-resolved and equilibrium descriptions at sufficiently slow interrogation rates. Conversely, at elevated frequencies, the model predicts a marked attenuation of the measured signal, capturing the experimentally observed drop in amplitude that results from kinetic constraints and interfacial limitations. This approach has been employed with considerable success in the interpretation of E-AB sensor data, particularly in the works of Plaxco and colleagues [*White et al. Langmuir* 2008, 24 (18), 10513–10518], where frequency-domain analysis enables differentiation between binding-induced and artefactual signal changes. Furthermore, the model facilitates comparison between different aptamer constructs, redox labels, or electrode configurations by extracting physically interpretable parameters such as k_{et} and f_{conf} .

While the phenomenological multi-exponential model introduced above provides a convenient and computationally tractable description of the frequency dependence of E-AB sensor signals, it does not explicitly incorporate the electrochemical kinetics that underlie electron transfer processes. As such, its parameters—though empirically useful—lack direct physical interpretation in terms of well-established electrochemical theory. To address this, we now extend the simulation framework using a more mechanistically grounded model based on the classical Butler–Volmer formalism.

The Butler–Volmer equation serves as the cornerstone of macroscopic electrochemical kinetics, describing how current density (j) evolves with applied overpotential (η) by accounting for both forward and reverse electron transfer reactions. It is given by:

$$j_{\text{BV}}(\eta) = j_0 \left[\exp\left(\frac{(1 - \alpha) F \eta}{RT}\right) - \exp\left(-\frac{\alpha F \eta}{RT}\right) \right],$$

where j_0 is the exchange current density proportional to the intrinsic electron transfer rate and the redox-active surface area, α is the charge-transfer coefficient typically ranging from 0.3 to 0.7 depending on the symmetry of the energy barrier, F is Faraday’s constant, R is the universal gas constant, T and is the absolute temperature. In this formulation, η represents the overpotential—the difference between the applied potential and the redox potential of the label—and modulates the balance between oxidation and reduction processes. However, in SWV, the potential waveform is pulsed and rapidly alternating, and as such, a static overpotential is not appropriate. To emulate the “rise-then-fall” pattern observed in experimental SWV amplitude-versus-frequency plots, we introduce a frequency-dependent

effective overpotential, $\eta_{\text{eff}}(f)$, that captures how the average electrochemical driving force evolves with the timescale of the perturbation:

$$\eta_{\text{eff}}(f) = \eta_0 \left(1 - \exp\left(-\frac{k_{\text{freq}}}{f}\right)\right),$$

This empirical relationship ensures that at low frequencies $f \ll k_{\text{freq}}$, the effective overpotential remains near zero, reflecting the fact that slow SWV perturbations allow the system to reach quasi-equilibrium at each potential step, minimising net current. As the frequency increases, η_{eff} asymptotically approaches η_0 , reflecting an increased driving force due to kinetic limitations in molecular or conformational rearrangements, effectively “locking in” a non-equilibrium overpotential.

Substituting the frequency-dependent effective overpotential $\eta_{\text{eff}}(f)$ into the Butler–Volmer framework allows us to simulate a non-monotonic frequency response with a well-defined physical basis. The full expression for the frequency-dependent current becomes:

$$I_{\text{net}}(f) = I_0 \cdot j_{\text{BV}}(\eta_{\text{eff}}(f)) \cdot \exp\left(-\frac{f}{f_{\text{conf}}}\right) \cdot \exp\left(-\frac{f}{f_{\text{others}}}\right).$$

This composite model captures several key physical features:

- The *initial rise* in current amplitude as the frequency increases is driven by the increase in $\eta_{\text{eff}}(f)$ enhancing the net electron transfer rate.
- The *peak response* occurs at an optimal frequency where both overpotential and conformational transitions are most favourably aligned.
- The *subsequent decay* at higher frequencies arises from the exponential suppression of the signal by limitations in aptamer conformational rearrangement f_{conf} and additional non-ideal effects f_{others} .

By fitting experimental frequency-response data to this model, researchers may extract meaningful physical parameters such as j_0 , η_0 and f_{conf} providing insights into the rate-limiting steps of signal transduction in E-AB systems. Importantly, this model unifies classical electrochemical theory with aptamer-specific dynamics, bridging the gap between thermodynamic and kinetic perspectives.

On a more microscopic and mechanistically rigorous level, Marcus theory provides a quantum-mechanical description of electron transfer, going beyond the thermodynamic perspective of Butler–Volmer kinetics. According to Marcus theory, the electron transfer rate k_{et} is governed not only by the free energy change ΔG° associated with the redox reaction but also by the reorganisation energy λ , which quantifies the energetic cost of rearranging the surrounding molecular and solvent environment to accommodate the charge transfer. The rate constant for electron transfer, under this theory, is expressed as:

$$k_{\text{et,base}} = A_{\text{Marcus}} \exp\left[-\frac{(\lambda + \Delta G^\circ)^2}{4\lambda k_B T}\right],$$

where A_{Marcus} is a pre-exponential factor related to electronic coupling and vibrational frequency, λ is the reorganisation energy (typically 0.5–1.0 eV in aqueous systems), ΔG° is the standard Gibbs free energy change for the reaction, T is the absolute temperature and k_B is Boltzmann’s constant.

One of the remarkable insights of Marcus theory is the prediction of an *inverted region*, in which increasing the driving force of the reaction (i.e., making ΔG° more negative) paradoxically leads to a decrease in the electron transfer rate. This counterintuitive regime is seldom encountered in typical redox reactions but becomes particularly relevant in systems with high reorganisation energies or strongly coupled states—scenarios that simpler models such as Butler–Volmer cannot account for. To adapt Marcus theory to a frequency-domain analysis relevant to Square Wave Voltammetry (SWV), we introduce a multiplicative activation term:

$$k_{et}(f) = \left[1 - \exp\left(-\frac{f}{k_{freq}}\right) \right] \cdot k_{et, base}$$

This term ensures that the effective electron transfer rate approaches zero in the low-frequency limit $f \rightarrow 0$ —reflecting the system’s near-equilibrium, reversible condition—and saturates to $k_{et, base}$ at intermediate-to-high frequencies. This frequency-responsive behaviour accounts for kinetic gating whereby only at faster interrogation rates does the electron transfer process become appreciably unbalanced, giving rise to a measurable net current.

The net frequency-dependent amplitude is then expressed as:

$$I_{net}(f) = I_0 \cdot k_{et}(f) \cdot \exp\left(-\frac{f}{f_{conf}}\right) \cdot \exp\left(-\frac{f}{f_{others}}\right)$$

As with the Butler–Volmer formulation, the parameter set $\{\Delta G^\circ, \lambda, f_{conf}, f_{others}\}$ can differ between the unbound and bound aptamer states, producing two distinct current–frequency profiles. In many experimental datasets, these two curves will intersect at some intermediate frequency, where the dynamic advantage of the bound state compensates for any thermodynamic disadvantage, and vice versa.

These physically grounded models, whether derived from Butler–Volmer kinetics or Marcus theory, offer a comprehensive frequency-domain framework that gracefully spans the full operating range of SWV interrogation. In the low-frequency limit, where the square wave perturbation is slow enough for the aptamer to fully relax between pulses, the signal amplitude approaches a steady-state value determined by the equilibrium binding state—i.e., close to I_{min} or I_{max} . At intermediate frequencies, systems with faster electron transfer (typically the bound state, in “signal-on” sensors) maintain higher signal amplitudes, while those with slower kinetics (e.g., unbound or obstructed conformations) begin to show attenuated responses. At very high frequencies, however, even the kinetically favourable states are penalised by conformational gating and capacitive or mass transport limitations, leading to a universal decline in current amplitude for both states.

Thus, while the classic fraction-bound model:

$$I = I_{min} + (I_{max} - I_{min}) \cdot \theta, \theta = \frac{[T]}{K_D + [T]}$$

describes how molecular recognition governs the equilibrium amplitude of the signal, the frequency-dependent Butler–Volmer and Marcus-based models offer additional layers of interpretation—revealing how kinetic limitations shape the amplitude as a function of square-wave interrogation rate. If measurements at partial target concentrations are available, these models can be interpolated by weighting the unbound and bound state amplitudes proportionally using the Hill–Langmuir formalism. However, in most practical scenarios,

measurements at just the two extremes (unbound and saturated states) suffice to elucidate how electron transfer kinetics differ between the aptamer conformations.

Finally, it is worth noting that the choice of experimental observable—whether peak current or integrated charge—does not alter the underlying physical model. Both metrics reflect the net electron transfer occurring within each cycle of the SWV waveform. So as long as a single, consistent amplitude is extracted per frequency per state, the data can be fitted using the same framework. Integrated charge measurements may prove more robust in capturing sluggish kinetics and capacitive delays, whereas peak current readings offer more direct correspondence with redox event intensity. The critical requirement is that each frequency point yields one amplitude for the unbound state and one for the bound state—these forming the fundamental dataset to which physically motivated models are fitted.

Conclusion

The development and refinement of electrochemical aptamer-based (E-AB) sensors have opened a versatile avenue for the detection of biologically and environmentally relevant analytes. While equilibrium binding models, such as the Hill–Langmuir isotherm, have provided a foundational understanding of how aptamer–target interactions modulate sensor response, they remain inherently limited in their ability to describe dynamic processes, especially under time-dependent electrochemical interrogation methods such as Square Wave Voltammetry (SWV). In such contexts, it is not solely the equilibrium fraction of bound aptamers that determines the observed signal, but also the rates at which electron transfer and associated molecular events occur in response to rapid perturbations in applied potential.

To address these limitations, this work introduces a framework that explicitly incorporates **frequency-dependent modifications** into two of the most widely used kinetic models in electrochemistry: the Butler–Volmer equation and Marcus theory. This innovation enables the modelling of current or charge responses under SWV conditions in a manner that reflects the distinct kinetic profiles of bound versus unbound aptamer states.

In the case of the Butler–Volmer formalism, a frequency-dependent effective overpotential, $\eta_{\text{eff}}(f)$, was introduced to modulate the net electron transfer rate as a function of SWV frequency. At low frequencies, η_{eff} remains near zero, capturing the quasi-equilibrium nature of electron transfer during slowly varying potential cycles. As frequency increases, η_{eff} asymptotically approaches a limiting value, η_0 , reflecting a progressively larger driving force due to limited relaxation time. This extension allows the model to reproduce the characteristic *rise–then–fall* profile observed experimentally, wherein current amplitude increases with frequency up to a certain point before declining due to gating and damping effects.

Complementarily, Marcus theory was adapted to the frequency domain by allowing the electron transfer rate k_{et} to evolve as a function of frequency via a saturating exponential function. This adjustment simulates how the system’s response transitions from a reversible regime, with negligible net current, to one dominated by irreversible kinetics where electron transfer is increasingly driven by non-equilibrium conditions. Importantly, Marcus theory introduces a conceptual depth absent from simpler models, including the possibility of observing the *inverted region*—a regime in which excessive driving force paradoxically reduces the rate of electron transfer. Although this regime may not be prevalent in typical E-AB configurations, the inclusion of Marcus-derived expressions enhances the theoretical robustness and interpretability of the simulation framework.

Beyond these two core models, the framework recognises the multiplicity of additional processes that influence E-AB sensor behaviour. These include conformational gating of the aptamer upon target binding, interfacial capacitive effects associated with double-layer charging, limitations in mass transport, and non-specific adsorption or surface passivation phenomena. Rather than complicating the core equations with excessive mechanistic detail, these effects are elegantly incorporated as independent exponential decay terms, parameterised by characteristic frequencies f_{conf} , f_{DL} , f_{mass} etc. This series-based formulation allows the total current or charge signal to be modulated by the compounded effects of all relevant kinetic barriers, capturing a more realistic representation of sensor performance across a wide range of frequencies.

A particularly important feature of the presented approach is that it facilitates a direct correlation between SWV frequency and kinetic differentiation of the bound versus unbound states. In “signal-on” E-AB sensors, the bound state typically exhibits faster electron transfer due to favourable spatial proximity of the redox reporter to the electrode. Consequently, as SWV frequency increases, the current associated with the bound state retains higher amplitude than that of the unbound state, which decays more rapidly due to its sluggish kinetics. This differential decay is the very signal exploited in E-AB sensor analysis and is precisely what is captured by the frequency-dependent extensions introduced here.

Moreover, while the amplitude extracted from SWV data may be presented either as peak current or as integrated charge, the modelling framework accommodates both metrics equivalently. So long as a consistent amplitude is extracted per frequency, the underlying principles and fitting procedures remain unchanged. Integrated charge may offer greater sensitivity to slow or broad processes, whereas peak current may be more robust for sharper, well-defined responses—yet both reflect the fundamental kinetics of the electron transfer process over the course of the SWV cycle.

In aggregate, this modelling strategy offers a unified platform for simulating and interpreting the performance of E-AB sensors under realistic, frequency-varying conditions. By bridging molecular recognition with kinetic electron transfer theory, it enables the simulation of current and charge profiles that align with empirical observations, all while maintaining physical interpretability of the parameters involved.

The entire theoretical developments and modelling strategies outlined herein have been implemented in a bespoke simulation tool named **Aptakin**. The *Aptakin* software provides a user-friendly environment for exploring how aptamer sequence, binding kinetics, electrode design, and SWV interrogation parameters affect sensor output. It supports both the Butler–Volmer and Marcus-based models with user-definable frequency parameters, as well as options to incorporate various exponential decay terms representing secondary processes. Aptakin has been designed with researchers in mind, offering a practical and flexible tool for the design, optimisation, and characterisation of next-generation E-AB sensors.

Through this work, we hope to advance both the theoretical and practical understanding of how frequency interrogation can be harnessed to reveal and exploit the subtle kinetic differences between binding states—thereby enhancing the precision, reliability, and utility of E-AB sensor technologies.

--- End of Script ---